SAHC'08 6th International Conference

STRUCTURAL ANALYSIS OF HISTORIC CONSTRUCTION

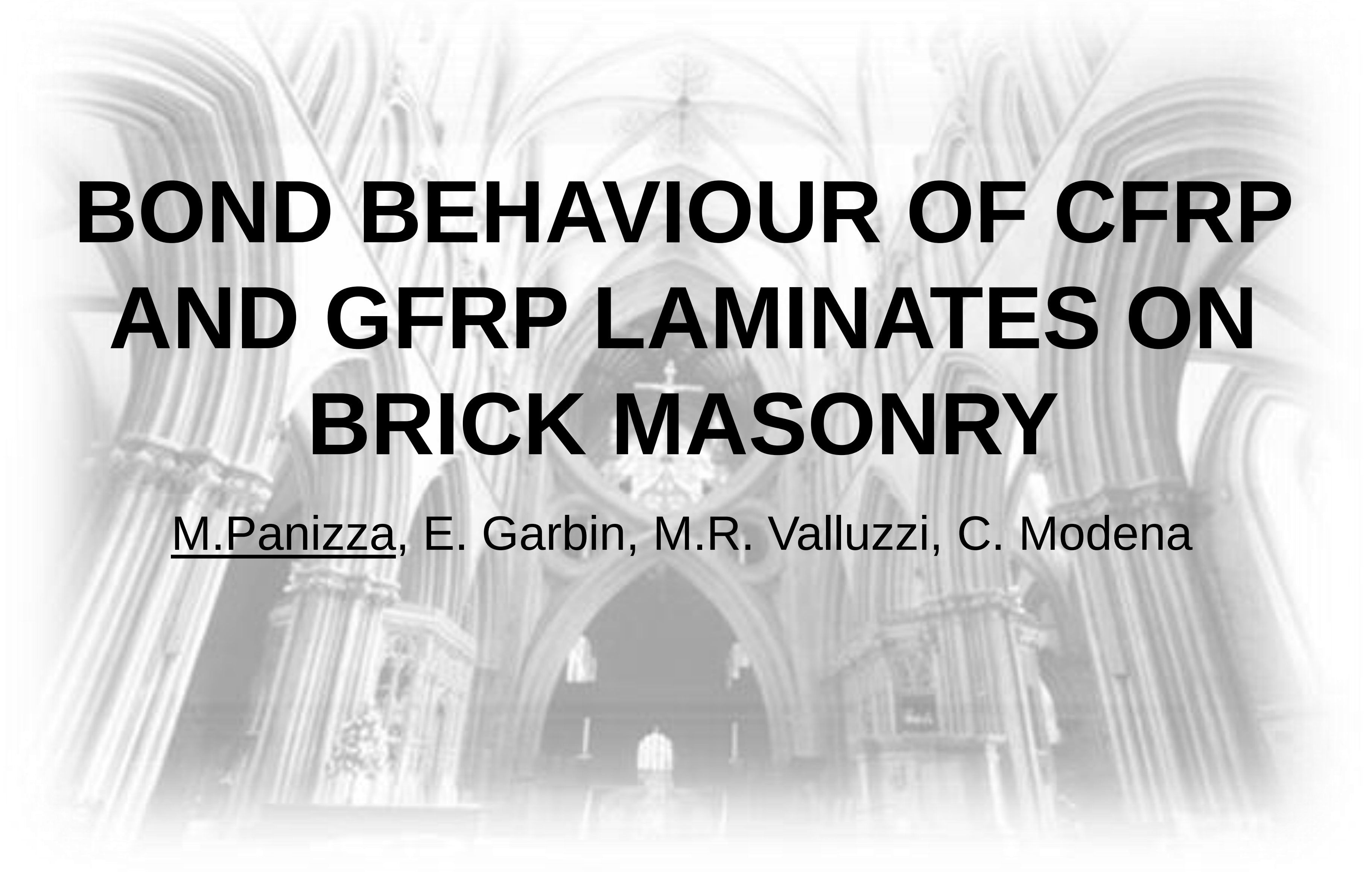

BOND BEHAVIOUR OF CFRP AND GFRP LAMINATES ON BRICK MASONRY

M.Panizza, E. Garbin, M.R. Valluzzi, C. Modena

Double-lap Shear tests: materials

Substrate: solid clay bricks

Mean cubic compressive strength	50.94	MPa
Mean direct tensile strength	2.37	MPa
Mean splitting tensile strength	3.99	MPa
Mean flexural tensile strength	5.46	MPa
Secant elastic modulus	16,100	MPa

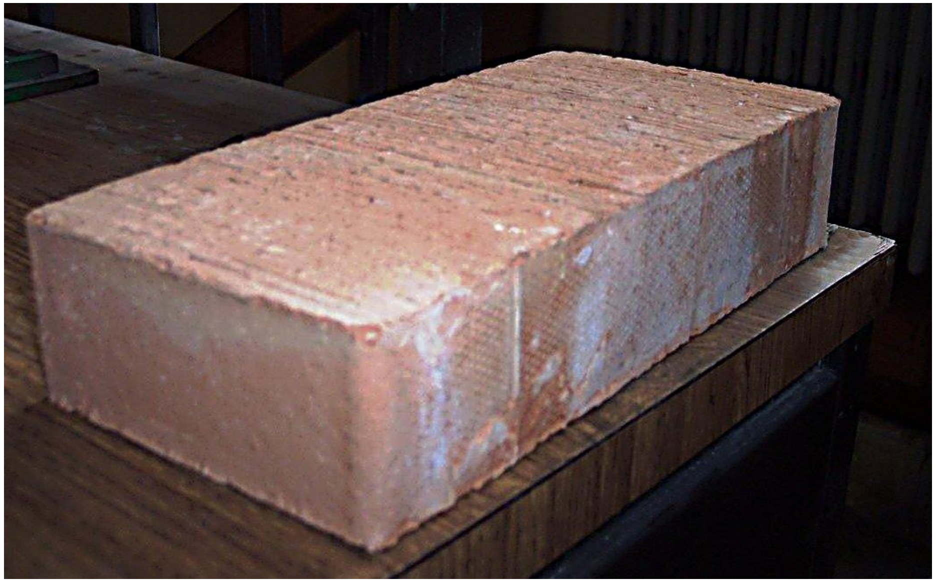

Reinforcement: Externally Bonded Carbon and Glass Textiles

Adhesive MBrace© Saturant		
Characteristic compressive strength	>80	MPa
Characteristic direct tensile strength	>50	MPa
Maximum tensile strain	2.5	%
Tensile elastic modulus	>3000	MPa
High-strength Carbon MBrace© C1-30		
Equivalent thickness	0.165	mm
Characteristic direct tensile strength	3430	MPa
Maximum tensile strain	1.5	%
Tensile elastic modulus	230,000	MPa
Alkali-resistant Glass MBrace© G60-AR		
Equivalent thickness	0.230	mm
Characteristic direct tensile strength	1700	MPa
Maximum tensile strain	2.8	%
Tensile elastic modulus	65,000	MPa

Double-lap Push-Pull Shear tests: set-up

- Two strips of FRP externally applied on the opposite wider surfaces of a single clay brick.
- Each strip 50 mm wide, bonded for 200 mm.
- Unbonded zone 30 mm long, in order to limit edge effects.
- Seven strain-gauges applied on the outer side of one strip.
- Tensile load applied to the FRP strips, brick forced to be compressed.
- Tests controlled by a displacement rate of 0.2 mm/min.

Sample's design layout

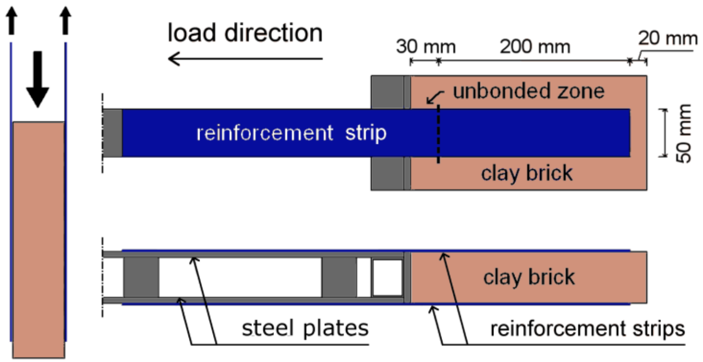

Test machine

Specimen ready for testing

Double-lap Shear tests: results

Typical failure: complete detachment of the reinforcement from brick's surface

Ripping of clay pieces

Curved cracks

Results in terms of failure load per unit width of the reinforcement:

Experimental results for carbon reinforcement.

Specimen	E_f MPa	P_u N	$P_u/2b'_f$ N/mm	σ_u MPa
ShC1	164,419	31,884	318.8	1932
ShC2	336,439	34,233	342.3	2075
ShC3	284,991	35,325	353.3	2141
ShC4	277,511	39,210	392.1	2376
ShC5	338,456	40,301	403.0	2442
Mean value	280,363	36,191	361.9	2193
Stand. dev.	70,696	3505		
COV	25.2 %	9.7 %		

Experimental results for glass reinforcement.

Specimen	E_f MPa	P_u N	$P_u/2b'_f$ N/mm	σ_u MPa
ShG1	50,934	23,380	233.8	1017
ShG2	87,014	27,940	279.4	1215
ShG3	80,545	27,300	273.0	1187
ShG4	102,598	26,400	264.0	1148
ShG5	84,842	28,360	283.6	1233
Mean value	81,035	26,676	266.9	1160
Stand. dev.	18,817	1985		
COV	23.2 %	7.4 %		

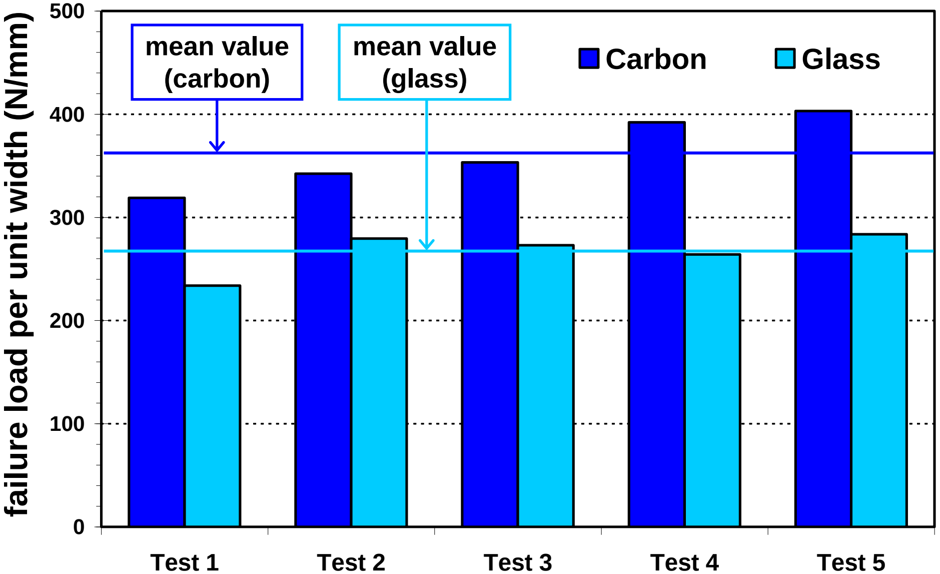

Peak loads vs axial stiffness: trend lines

First analysis: **evaluation of trend lines for the failure loads per unit width of the reinforcement as function of the axial stiffness $E_f t_f$ measured through the strain gauges applied on the unbonded region.**

Second analysis: evaluation of trend lines as before, but fixing the exponent $c_2 = 0.5$ (Square Root).

Regression coefficient for GFRP are slightly higher than CFRP (around 16%), and this could be significant for the fracture energy evaluation.

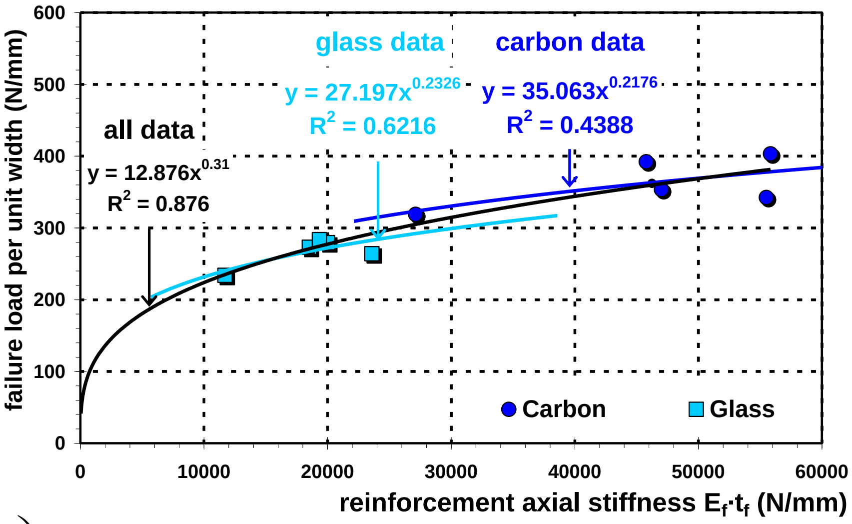

$$\left(\frac{P_u}{2b'_f}\right) = c_1\left(E_f t_f\right)^{c_2}$$

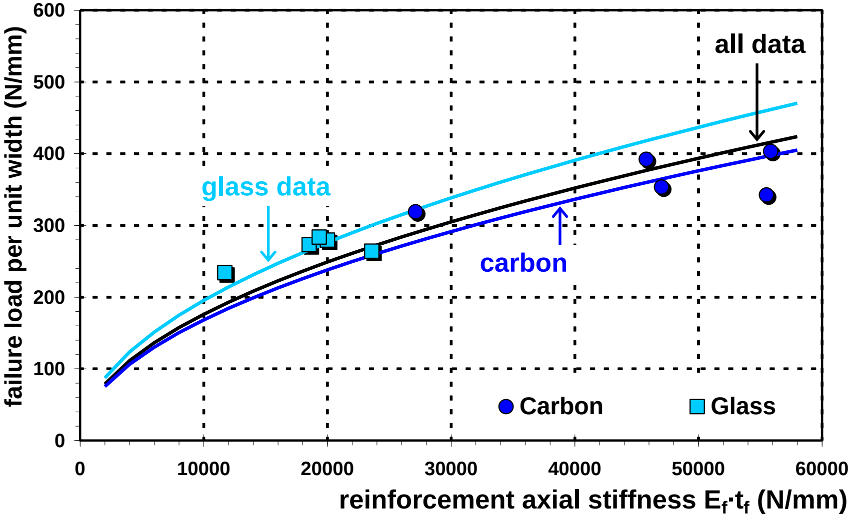

Data set	c_1	c_2	R^2
All data	12.876	0.310	0.876
Glass data only	27.197	0.234	0.622
Carbon data only	35.063	0.218	0.439
All data (Square Root)	1.759	*0.5*	n.a.
Glass data (Square Root)	1.953	*0.5*	n.a.
Carbon data (Square Root)	1.681	*0.5*	n.a.

Prediction of strength through available models

Twenty-one predictive models, developed to estimate the failure load P_u of the composite-to-concrete bonded joint, were applied in order to make a comparison with the experimental results of the tests on clay substrate.

	CFRP		GFRP	
Model	$P_u / 2b'_f$ N/mm	Error	$P_u / 2b'_f$ N/mm	Error
Tanaka	166	-54.0%	166	-37.6%
Hiroyuki and Wu	158	-56.2%	158	-40.6%
Maeda	254	-29.7%	174	-34.9%
Khalifa	248	-31.4%	170	-36.2%
Yang	192	-47.0%	143	-46.3%
Sato	415	+14.6%	116	-56.5%
Iso	271	-25.1%	161	-39.5%
Izumo	557	+53.9%	224	-15.9%
Neubauer and R.	283	-21.8%	179	-32.7%
Chen and Teng	245	-32.2%	156	-41.6%
Monti et al.	321	-11.3%	204	-23.6%
Lu et al. Bilinear	220	-39.3%	139	-47.7%
Brosens and V. G.	359	-0.9%	228	-14.7%
CNR-DT 200	263	-27.4%	167	-37.5%
Nakaba et al.	350	-3.3%	222	-16.7%
Savoia et al.	328	-9.4%	208	-22.0%
Neubauer and R.	266	-26.4%	169	-36.6%
Dai and Ueda (1)	326	-9.9%	207	-22.5%
Dai and Ueda (2)	322	-11.0%	202	-24.2%
Lu et al. Precise	220	-39.3%	139	-47.7%
Lu et al. Simplif.	220	-39.3%	139	-47.7%
Mean experim.	362	–	267	–

- ☐ **Large differences from model to model: they vary between 44% ÷ 154% of mean experimental P_u (CFRP) and 43% ÷ 85% (GFRP);**
- ☐ **all the predictions (closer to test results in case of CFRP than GFRP), except two in case of CFRP, underestimate the mean experimental P_u.**

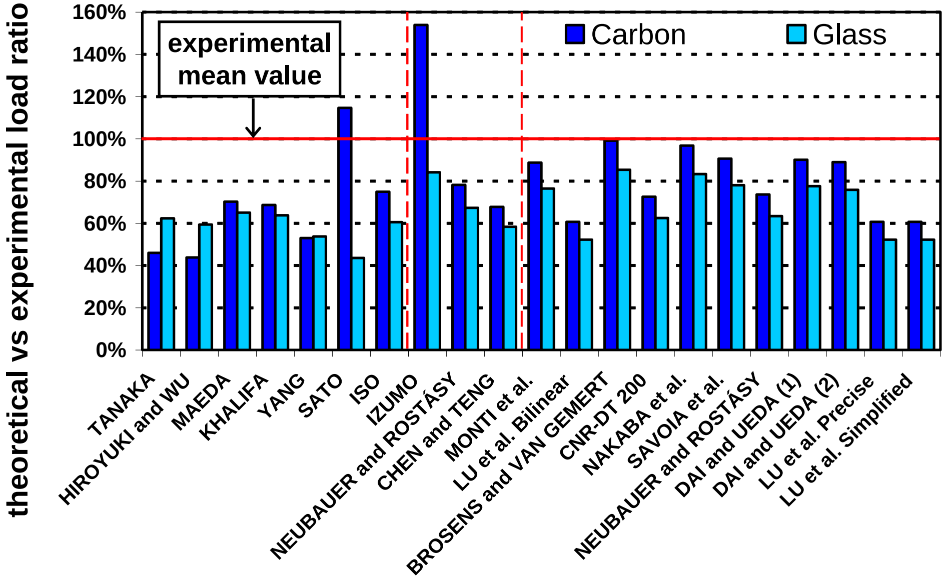

Calibration of the fracture energy G_f

The interface fracture energy mode II, G_f, is defined as the definite integral of the tangential stress τ, expressed as function of the mutual slip of composite and substrate, s.

Similar analytical relations between G_f and the failure load have been considered:

$$G_f = \int_0^\infty \tau(s)\,ds$$

Täljsten (1996):

$$P_u = b_f \sqrt{\frac{2E_f t_f G_f}{1+\alpha_T}};\quad \alpha_T = \frac{E_f t_f}{E_c t_c}$$

Yuan and Wu (1999):

$$P_u = b_f \sqrt{\frac{2E_f t_f G_f}{1+\alpha_W}};\quad \alpha_W = \frac{b_f E_f t_f}{b_c E_c t_c}$$

Recent works:

$$P_u = b_f \sqrt{2E_f t_f G_f}$$

By applying the first and second relation to the experimental data of this work, it emerges that taking or not into account the parameters α_T or α_W leads to a difference lower than 2%.

Therefore the third equation was applied to derive a first calibration of the mean G_f.

A second calibration was based on the coefficient c_1 of the second set of trend lines (S.R. fitting) formerly exposed.

$$\text{from S.R. fitting}: P_u = c_1 \left(E_f t_f\right)^{0.5}$$

- ❑ **There is no significant difference between the first and the second calibration of the fracture energy;**
- ❑ **The estimated value, for glass reinforcement, is around 35% higher than carbon one.**

Reinforcement type	G_f from Eq. 7 N/mm	G_f from S.R. fit N/mm
Carbon fibers	1.42	1.41
Glass fibers	1.91	1.91

Calibration of a bond-slip law (1)

To calibrate the bond-slip law on the experimental results, this combined approach was adopted: tangential stress and interface slip points (τ–s) were obtained from strain-gauges monitoring, while the fracture energy value, G_f, was calculated from failure loads.

The main relations between reinforcement strain ε, interface tangential stress τ and slip s, obtained from simple equilibrium and compatibility considerations supposing to disregard the slip component of the substrate (sufficiently stiffer than composite) are:

$$\frac{d\varepsilon(x)}{dx} = \frac{1}{E_f t_f}\tau(x)$$

$$\varepsilon(x) = \frac{ds(x)}{dx} \Rightarrow s(x) = \int_0^x \varepsilon(x)dx$$

$$\frac{d^2 s(x)}{dx} - \frac{1}{E_f t_f}\tau(x) = 0$$

To calculate, from strain measured in discrete positions along the reinforcement, the corresponding tangential stress and slip values, formulas (Valluzzi et al. 2003) that allow to manipulate data from devices not uniformly spaced were used.

$$\boxed{\tau_i = \tau(x_i) = \frac{1}{2}E_f t_f \left(\frac{\varepsilon_i - \varepsilon_{i+1}}{x_{i+1} - x_i} + \frac{\varepsilon_{i-1} - \varepsilon_i}{x_i - x_{i-1}} \right)}$$

$$\boxed{s_i = s(x_i) = s_{i+1} + \frac{1}{2}(\varepsilon_i + \varepsilon_{i+1})(x_{i+1} - x_i)}$$

Calibration of a bond-slip law (2)

It is assumed that the bond-slip law should show an ascending segment and a softening behaviour.

Instead of using two different mathematical expressions for the ascending and the descending branch, a single function was chosen; although there could be a slight loss of adherence to experimental data, it reduces the required parameters making easier the fitting process.

The proposed law, easy to integrate and derive (UniPd curve):

BASIC FUNCTION (depending on two parameters):

$$\tau(s) = A \cdot s \cdot e^{-Bs}$$

BUT, knowing that $\int_0^\infty \tau ds = G_f$ **=> reduction of free parameters**

$$\tau(s) = B^2 G_f \cdot s \cdot e^{-Bs}; \qquad \tau(s) = \frac{G_f}{s_0^2}(s) e^{-\frac{s}{s_0}};$$

NORMALIZED EXPRESSION:

$$\boxed{\frac{\tau(s)}{\tau_{\max}} = \left(\frac{s}{s_0}\right) e^{\left(1-\frac{s}{s_0}\right)}}$$

After the optimization of the UniPd curves, in case of carbon reinforcement and glass one, it was possible to calibrate a bilinear law.

BILINEAR FUNCTION:

$$\tau(s) = \begin{cases} \tau_{\max}\left(s/s_0\right) & 0 \le s < s_0 \\ \tau_{\max}\left(\left(s_f - s\right)/\left(s_f - s_0\right)\right) & s_0 \le s < s_f \\ 0 & s \ge s_0 \end{cases}$$

Calibration of a bond-slip law (3)

Moreover, the main parameters of the calibrated curves, namely the fracture energy G_f, the maximum tangential stress τ_{max} and its related slip s_0, and the ultimate slip s_f (if defined), have been compared with the parameters obtained through the predictive models able to provide them.

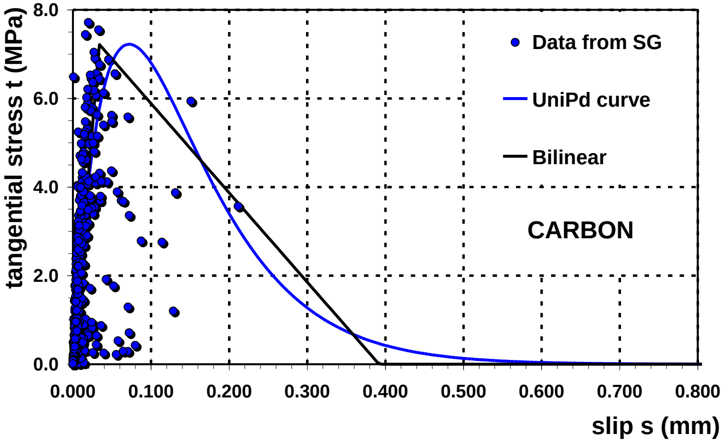

CARBON REINFORCEMENT

$$\tau(s) = 7.22\left(\frac{s}{0.072}\right)e^{\left(1-\frac{s}{0.072}\right)}$$

GLASS REINFORCEMENT

$$\tau(s) = 6.33\left(\frac{s}{0.111}\right)e^{\left(1-\frac{s}{0.111}\right)}$$

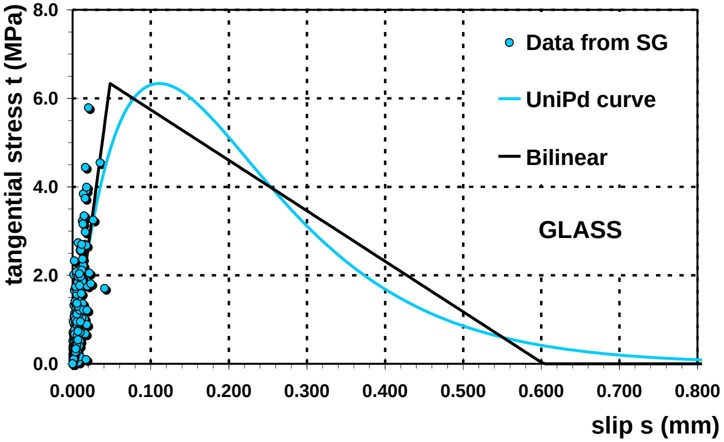

CARBON	G_f N/mm	τ_{max} MPa	s_0 mm	s_f mm
UniPd fitting	1.42	7.22	0.072	-
Bilinear fitting	1.42	7.22	0.034	0.392
Monti et al.	1.11	5.37	0.046	0.415
Lu et al. Bilinear	0.52	3.73	0.048	0.280
Brosens and V. G.	1.39	2.71	0.012	1.025
CNR	0.75	7.46	0.056	0.200
Nakaba et al.	1.32	7.08	0.065	-
Savoia et al.	1.16	7.08	0.051	-
Neubauer and R.	0.77	5.69	0.270	-
Dai and Ueda (1)	1.15	8.58	0.103	-
Dai and Ueda (2)	1.12	6.41	0.061	-
Lu et al. Precise	0.52	3.73	0.054	-
Lu et al. Simplif.	0.52	3.73	0.048	-
GLASS				
UniPd fitting	1.91	6.33	0.111	-
Bilinear fitting	1.91	6.33	0.048	0.603
Monti et al.	1.11	5.37	0.046	0.415
Lu et al. Bilinear	0.52	3.73	0.048	0.280
Brosens and V. G.	1.39	2.71	0.012	1.025
CNR	0.75	7.46	0.056	0.200
Nakaba et al.	1.32	7.08	0.065	-
Savoia et al.	1.16	7.08	0.051	-
Neubauer and R.	0.77	5.69	0.270	-
Dai and Ueda (1)	1.15	7.10	0.107	-
Dai and Ueda (2)	1.10	5.69	0.067	-
Lu et al. Precise	0.52	3.73	0.054	-
Lu et al. Simplif.	0.52	3.73	0.048	-

Double-lap Push-pull S. T: CONCLUSIONS

- **The results of the tests performed on clay bricks reinforced by CFRP and GFRP show a better performance of carbon reinforcement than glass one (around 36% higher in the first case);**
- **all the applied predictive models (except two in case of CFRP) underestimate the results of the tests; they seem to work better (except two in case of GFRP) for the carbon reinforcement. However, the strength predictions vary into an wide range (44% ÷ 154% of experimental mean failure load for CFRP, 43% ÷ 85% for GFRP);**
- **from the measured failure loads, different fracture energy values have been derived, around 35% higher in case of glass reinforcement than carbon one;**

Double-lap Push-pull S. T: CONCLUSIONS

- **to analyze stress and slip from not uniformly spaced strain-gauges measurement, discrete equations have been used, consistent with central finite difference methods;**
- **a mathematical function, easy to integrate and derive, is proposed as bond-slip law. This function has been fitted in case of both carbon and glass reinforcement; beside these fittings, two bilinear functions have been also calibrated. The optimized functions seem to show an interface local behaviour of CFRP slightly stiffer than GFRP;**
- **these tests are a first step in order to take into account, in the future, the role of the mortar joints, characteristic of masonry structures;**
- **the reliability of the experimental setup needs to be verified; despite of its simplicity, the actual distribution of the load should be more clarified.**

BOND BEHAVIOUR OF CFRP AND GFRP LAMINATES ON BRICK MASONRY

THANK YOU
FOR THE ATTENTION

M.Panizza, E. Garbin, M.R. Valluzzi, C. Modena

Department of Structural and
Transportation Engineering
University of Padova – ITALY